HHS Public Access

Author manuscript

Hepatology. Author manuscript; available in PMC 2022 July 06.

Published in final edited form as:

Hepatology. 2021 April ; 73(4): 1381–1398. doi:10.1002/hep.31448.

MiR-125b Loss Activated HIF1α/pAKT Loop, Leading to Transarterial Chemoembolization Resistance in Hepatocellular Carcinoma

Xiyang Wei[1,*], **Lei Zhao**[2,*], **Ruizhe Ren**[1], **Fubo Ji**[1], **Shuting Xue**[1], **Jianjuan Zhang**[1], **Zhaogang Liu**[2], **Zhao Ma**[2], **Xin W. Wang**[3], **Linda Wong**[4], **Niya Liu**[1], **Jiong Shi**[5], **Xing Guo**[1], **Stephanie Roessler**[6], **Xin Zheng**[7], **Junfang Ji**[1]

[1]MOE Key Laboratory of Biosystems Homeostasis & Protection, Life Sciences Institute, Zhejiang University, Hangzhou, China

[2]Shandong Cancer Hospital and Institute, Shandong Cancer Hospital of Shandong First Medical University, Jinan, China

[3]Liver Cancer Program and Laboratory of Human Carcinogenesis, Cancer for Cancer Research, National Cancer Institute, Bethesda, MD

[4]University of Hawaii Cancer Center, Honolulu, HI

[5]Department of Pathology, Nanjing Drum Tower Hospital, the Affiliated Hospital of Nanjing University Medical School, Nanjing, China

[6]Institute of Pathology, University Hospital Heidelberg, Heidelberg, Germany

[7]Ezkit LLC, Honolulu, HI

Abstract

BACKGROUND AND AIMS: Transarterial chemoembolization (TACE) is a standard locoregional therapy for patients with hepatocellular carcinoma (HCC) patients with a variable overall response in efficacy. We aimed to identify key molecular signatures and related pathways leading to HCC resistance to TACE, with the hope of developing effective approaches in preselecting patients with survival benefit from TACE.

APPROACH AND RESULTS: Four independent HCC cohorts with 680 patients were used. MicroRNA (miRNA) transcriptome analysis in patients with HCC revealed a 41-miRNA signature related to HCC recurrence after adjuvant TACE, and miR-125b was the top reduced miRNA in patients with HCC recurrence. Consistently, patients with HCC with low miR-125b

ADDRESS CORRESPONDENCE AND REPRINT REQUESTS TO: Junfang Ji, Ph.D., MOE Key Laboratory of Biosystems Homeostasis & Protection, Life Sciences Institute, Zhejiang University, 866 Yuhangtang Road, Hangzhou, Zhejiang Province, 310058, China, junfangji@zju.edu.cn, Tel.: +86 571 88208956.

*The authors contributed equally to this work.

Author Contributions: Conception and design: X.W., and J.J.; Development of methodology: X.W., and J.J.; Acquisition of data: X.W., L.Z., R.R., F.J., S.X., J.Z., Z.L., J.J.; Analysis and interpretation of data: X.W., L.Z., X.W., S.R., X.Z., J.J.; Clinical data collection, and pathological assessment: L.Z., Z.L., Z.M., J.S.; Writing, review, and/or revision of the manuscript: X.W., S.R., X.W., L.W., X.Z., J.J.; Administrative, technical, or material support: X.Z., N.L., X.G., J.J.; Study supervision: J.J.

Potential conflict of interest: Dr. Wong is on the speakers' bureau for Eisai.

Additional Supporting Information may be found at onlinelibrary.wiley.com/doi/10.1002/hep.31448/suppinfo.

expression in tumor had significantly shorter time to recurrence following adjuvant TACE in two independent cohorts. Loss of miR-125b in HCC noticeably activated the hypoxia inducible factor 1 alpha subunit (HIF1α)/pAKT loop *in vitro* and *in vivo.* miR-125b directly attenuated HIF1α translation through binding to *HIF1A* internal ribosome entry site region and targeting YB-1, and blocked an autocrine HIF1α/platelet-derived growth factor β (PDGFβ)/pAKT/HIF1α loop of HIF1α translation by targeting the PDGFβ receptor. The miR-125b-loss/HIF1α axis induced the expression of CD24 and erythropoietin (EPO) and enriched a TACE-resistant CD24-positive cancer stem cell population. Consistently, patients with high CD24 or EPO in HCC had poor prognosis following adjuvant TACE therapy. Additionally, in patients with HCC having TACE as their first-line therapy, high EPO in blood before TACE was also noticeably related to poor response to TACE.

CONCLUSIONS: MiR-125b loss activated the HIF1α/pAKT loop, contributing to HCC resistance to TACE and the key nodes in this axis hold the potential in assisting patients with HCC to choose TACE therapy.

Primary liver cancer is the second most deadly human malignancy in men, and about 80% of cases are hepatocellular carcinoma (HCC). HCC exhibits strong heterogeneity, and its 5-year overall survival rate remains below 20%.[1] One of the key reasons for the overall poor survival is the variable benefit from current therapeutic treatments due to the HCC heterogeneity.[2]

According to the American Association for the Study of Liver Diseases and European Association for the Study of the Liver HCC guidelines, transarterial chemoembolization (TACE) is a recommended first-line therapy for patients with intermediate stage (Barcelona Clinic Liver Cancer (BCLC]-B stage) HCC[3,4] and a neoadjuvant therapy to bridge patients with early-stage HCC to liver transplantation or downstage HCC to respectability.[5–7] TACE is also used as an adjuvant therapy after surgical resection to reduce tumor recurrence in many Asian countries.[8,9] It is a procedure involving intra-arterial infusion of chemotherapeutic drugs such as doxorubicin, followed by infusion embolic particles to induce cell death and create a localized ischemic injury. Currently, the survival outcome of patients managed with this technique is variable, and only some patients exhibit a survival benefit from adjuvant TACE therapy.[7,8,10] Imaging of altered tumor areas after TACE therapy based on the modified Response Evaluation Criteria in Solid Tumors (mRECIST) criteria could evaluate the overall survival for HCCs under BCLC-B stage.[5] However, it lacks the power to identify patients with HCC who would benefit from TACE before therapy.

To develop an effective approach predicting the survival benefit from TACE in advance, it is essential to thoroughly understand the mechanism of HCC resistance to TACE both *in vitro* and *in vivo*. MiRNAs present diverse roles in tumorigenesis, tumor recurrence and therapeutic response, as well as provide potential clinical tools in diagnosis, companion diagnostics, and prognosis in cancer.[11–16] Human miR-125b-5p (miR-125b) is the orthologue of *lin-4* in *C. elegans,* the first miRNA discovered and regulating *C. elegans* development. Mature miR-125b is produced from two precursors, mir-125b-1 on chromosome 11q23 and mir-125b-2 on chromosome 21q21, and widely participates in various biological processes, such as proliferation, differentiation, cell death, as well as

tumor progression including HCC.[17,18] Patients with HCC with low miR-26 level in their tumors have poor prognosis but gain survival benefit from adjuvant interferon alpha therapy.[12,13] We therefore hypothesized that miRNAs and their related signaling pathways may contribute to HCC resistance to TACE.

Materials and Methods

HCC COHORTS, TRANSCRIPTOMIC DATA SETS

A total of four cohorts were used in this study. Cohort 1 included 241 Chinese HCC cases with tumor resection, among which 241 cases had available miRNA transcriptome data (GSE6857) and 184 cases had messenger RNA (mRNA) transcriptome data for paired tumor and nontumor specimens (GSE14520).[19–21] Cohort 2 consisted of 61 patients with HCC with available archived formalin-fixed paraffin-embedded (FFPE) HCC tissues. They were from Shandong Cancer Hospital and Institute, and the institutional review board approved the use of these FFPE tissues and waived the requirement for informed consent (Supporting Table S1). Cohort 3 included 367 HCC cases with miRNA and mRNA sequencing data in all HCC tissues and 50 normal liver tissues from The Cancer Genome Atlas. Cohort 4 consisted of 11 patients with BCLC-B/C stage HCC, who had TACE as their first-line therapy (Supporting Table S2). Their plasma, clinical parameters, and imaging assessment were collected. All plasma samples were prospectively collected before TACE from the End-Results program of Shandong Cancer Hospital and Institute, and their use was approved as exempt research by their institutional review board.

CELL LINES AND HLE^{125KO} CELLS

Human liver cancer cell lines (HuH7, HLE, HuH1, and HLF), hepatic stellate cell line (LX2), intrahepatic cholangiocarcinoma cell line (RBE), lung carcinoma cell line (A549), embryonic kidney cell line (293T), and mouse embryo fibroblast cell line (NIH3T3) were routinely cultured in our lab.[22,23] HuH7, HLE, HuH1, HLF, and RBE were originally from JCRB (Tokyo, Japan). A549, NIH3T3, and 293T were from ATCC (Manassas, VA). LX2 and HL-7702 were from the Chinese Academy of Sciences (Shanghai, China).

MiR125 knockout HCC cells were generated using the CRISPR/Cas9 system. Single-guide RNAs were designed using an online web tool (http://crispr.mit.edu) to target the precursor mir-125b-1 and mir-125b-2, and cloned into pSpCas9(BB)-2A-Puro vector after being synthesized. After transfection, positive miR-125b knockout clones were screened. Only clones with alteration of both mir-125b-1 and mir-125b-2 were selected.

The rest of materials and methods are included in the Supporting Information.

Results

AN miRNA-SIGNATURE WAS RELATED TO HCC RECURRENCE AFTER ADJUVANT TACE

The diagnosis of HCC can be made based on typical imaging features without biopsy, which limited the possibility of acquiring tumor specimens from patients with BCLC-B-stage HCC, to explore molecular mechanisms of tumor progression after TACE *in vivo*. However, we were able to analyze two cohorts including patients with adjuvant TACE

after surgical tumor resection (Fig. 1A and Supporting Table S1). Consistent with previous reports,[8,9,24,25] adjuvant TACE slightly but not significantly improved prognosis of HCC cases in both cohorts (Supporting Fig. S1A,B). No significant difference was observed in terms of clinical characteristics between patients with or without adjuvant TACE in both cohorts (Supporting Table S3).

Adjuvant TACE after HCC resection aimed to reduce tumor recurrence in the cohorts studied. Recurrence within 2 years after tumor resection was related to early dissemination of the primary tumor.[9,26] To explore miRNA signatures related to tumor progression after TACE, tumor miRNA profiles from patients with adjuvant TACE after tumor resection were compared between HCCs, with recurrence within 2 years (HCC^{Recur}, n = 21) and HCCs without recurrence after 2 years ($HCC^{no\text{-}Recur}$, n = 29), in cohort 1 (Fig. 1A). There were 250 nonredundant miRNAs, with a total of 615 miRNA probes in these miRNA profiles, which were collected in tumors at surgical resection. Clinical characteristics between patients with HCC^{Recur} and $HCC^{no\text{-}Recur}$ showed no significant difference (Supporting Table S4). MiRNA profiling comparison revealed 59 probes with significant difference between the two groups (Fig. 1B). Clustering analysis using 59 miRNA probes divided 62 cases with adjuvant TACE in cohort 1 into three groups with distinct prognosis ($P < 0.01$), shown by either tumor to recurrence or overall survival (Fig. 1C). As a control, these probes did not significantly associate with the prognosis of either HCC cases without TACE (Supporting Fig. S1C,D) or other HCC cases (Supporting Fig. S1E,F). Thus, this signature was uniquely related to the apparent overall response to adjuvant TACE after tumor resection in HCC.

PATIENTS WITH HCC WITH HIGHER LEVELS OF miR-125b GAINED SIGNIFICANT SURVIVAL BENEFIT FROM ADJUVANT TACE

The identified 59 probes correspond to 41 unique miRNAs, of which the top reduced one in HCC^{Recur} cases was miR-125b-5p (miR-125b) (Supporting Table S5). In HCC, miR-125b was down-regulated in tumor and exhibited a tumor-suppressor role.[18,27] In HCCs with adjuvant TACE, miR-125b was significantly down-regulated in tumor tissues compared with nontumors from HCC^{Recur} cases, but not in $HCC^{no\text{-}Recur}$ cases (Fig. 1D). When the median level of miR-125b was used as the cutoff for patients with adjuvant TACE, HCCs with higher levels of miR-125b in the tumor presented a significantly longer time to recurrence and longer overall survival time, compared to HCCs with lower levels of miR-125b (Fig. 1E). As a control, miR-125b did not predict prognosis in HCC cases without adjuvant TACE (Fig. 1E), although its expression showed no difference between HCCs with or without adjuvant TACE (Supporting Fig. S1G).

The miR-125b-predicting survival benefit from adjuvant TACE was validated in an independent HCC cohort (cohort 2). In this cohort, 37 of 61 cases had adjuvant TACE after tumor resection, and clinical characteristics exhibited no difference between HCCs with and without adjuvant TACE (Supporting Table S3). As shown in Fig. 1F, HCCs with a higher level of miR-125b consistently had a significant survival benefit from adjuvant TACE, whereas miR-125b expression was not related to survival in HCCs without adjuvant TACE. Microvascular invasion (MVI) in primary resected HCCs was related to the patient's outcome. One group reported that the absence of MVI was associated with improved

outcome for patients with HCC with adjuvant TACE after tumor resection,[28] although the other mentioned that patients with MVI showed improved prognosis through a meta-analysis.[29] As shown in Supporting Fig. S2A–D, the absence of MVI was consistently associated with poor prognosis in patients without adjuvant TACE of both cohorts, but not in patients with adjuvant TACE. Meanwhile, miR-125b showed no differential expression between patients with and without MVI in their primary resected HCCs (Supporting Fig. S2E,F). Taken together, a higher miR-125b expression in HCC was associated with a favorable response to adjuvant TACE after tumor resection. This was not due to the role of miR-125 in subselecting patients with good prognosis, but in potentially selecting a subgroup of patients with certain TACE-related tumor biology alteration.

LOSS OF MiR-125b INCREASED HCC RESISTANCE TO DOXORUBICIN UNDER HYPOXIA AND ENRICHED CD24$^+$ CELL POPULATION

To investigate the potential TACE resistance–related cellular and molecular biology in HCC cells with low miR-125b expression, we established miR-125b knockout cells using the CRISPR-Cas9 system in HLE cells with relatively high levels of miR-125b (Fig. 2A). As shown in Fig. 2B, miR-125b knockout HLE cells were established using two paired guide RNAs to specifically target both miR-125b precursors (mir-125b-1 on Chr.11q23 and mir-125b-2 on Chr.21q21), termed as HLE^{125bKO}. In HLE^{125bKO} cells, both mir-125b-1 and mir-125b-2 were successfully interfered as verified by DNA sequencing and PCR (Supporting Fig. S3A), and the miR-125b level was about under detectable (Fig. 2C).

TACE is a procedure involving treatment with chemotherapeutic drugs and embolization, exposing cells to high concentrations of chemo drugs such as doxorubicin and hypoxia. Thus, we exposed cells to 1% of O_2 and different doses of doxorubicin to mimic *in vivo* TACE treatment. With doxorubicin treatment under hypoxia, HLE^{125bKO} cells exhibited a significantly higher cell viability compared with HLE^{WT} cells, which was reduced by overexpressing miR-125b (Fig. 2C). Consistent data were obtained in Huh7 cells (Fig. 2D). Furthermore, after exposure under 1%O_2 and 0.1 μM of doxorubicin, HLE^{125bKO} cells exhibited significantly less cell apoptosis compared with HLE^{WT} cells, which was increased by forced expression of miR-125b (Fig. 2E). Comparable data were also obtained in Huh7 (Fig. 2F). Together, HCC cells with low levels of miR-125b presented cell resistance to doxorubicin under hypoxia *in vitro*.

Hepatic cancer stem cells (CSCs) are involved in chemo-resistance, and we previously found miR-125b to be one of the miRNAs with reduced levels in CSC$^+$ HCCs.[22,30] Thus, miR-125b might suppress hepatic CSC populations and consequently regulate cell resistance to TACE. Compared with HLE^{WT} cells, HLE^{125bKO} formed significantly more spheroids, which were reduced by overexpressing miR-125b (Fig. 3A). Consistent data were obtained in HuH7. We further examined the alteration of different hepatic CSC populations after overexpression of miR-125b in HCC cells. As shown in Fig. 3B, overexpressed miR-125b in Huh7 cells led to a significant reduction of CD24$^+$ and epithelial cell adhesion molecule (EpCAM$^+$) CSC populations, a minor reduction of CD133$^+$ populations, but no reduction of CD44$^+$ cells. HLE^{WT} cells were negative for EpCAM, CD24 and CD133 staining, whereas HLE^{125bKO} cells produced a substantial amount of CD24$^+$ populations, which

could be reduced by overexpression of miR-125b. Compared with HLE^{WT}, HLE^{125bKO} cells also exhibited a moderate increase of $EpCAM^+$ and $CD133^+$ populations, which were not suppressed by miR-125b overexpression. Comparable data were obtained in patients with HCC. Levels of CD24, CD133, and EpCAM CSC biomarkers were significantly higher in the $miR\text{-}125b^{low}$ group compared with that in the $miR\text{-}125b^{high}$ group, but the expression of CD90 and CD44 CSC biomarkers were not (Fig. 3C and Supporting Fig. S3B,C). These results indicate an important role of miR-125b in restricting several CSC populations, especially $CD24^+$ cells in different HCC cells.

Under 1%O_2 and 0.1 μM Dox, $CD24^+$, $EpCAM^+$, and $CD133^+$ HuH7 cells formed more colonies than their corresponding negative cells (Fig. 3D). Significantly, sorted $CD24^+$ Huh7 cells formed the most colonies, while $CD24^-$ cells formed the least colonies, among all of the sorted CSC biomarker negative or positive cells ($CD24^+$ vs. $CD24^-$, 483 ± 14 vs. 90 ± 6; Fig. 3D). Consistently, isolated $CD24^+$ cells showed a significantly higher cell viability after exposure to a different dose of doxorubicin under hypoxia, compared with $EpCAM^+$, $CD133^+$ HuH7 cells, as well as control Huh7 cells (Fig. 3E). Comparable data were also noticed in HuH1 cells, and HLE^{125bKO} cells that isolated $CD24^+$ cells formed significant more colonies compared with their corresponding $CD24^-$ cells after exposure to doxorubicin under hypoxia (Fig. 3F). Moreover, under three different conditions, including doxorubicin plus hypoxia, only doxorubicin, as well as neither doxorubicin nor hypoxia, $CD24^+$ Huh7 cells formed the most colonies, while $CD24^-$ cells formed the least colonies when exposed to doxorubicin under hypoxia (Supporting Fig. S3D). As a control, neither $EpCAM^+$ nor $CD133^+$ exhibited such a noticeable difference when exposed to these three conditions. Thus, $CD24^+$ HCC cells possessed a significantly high survival ability after exposure to doxorubicin under hypoxia. Together, loss of miR-125b in HCC cells led to an enriched $CD24^+$ population, mounting cell resistance to doxorubicin under hypoxia, which mimicked *in vivo* TACE treatment.

THE ENRICHMENT OF $CD24^+$ CELLS BY MiR-125b LOSS WAS DUE TO AN INCREASED HIF1α LEVEL

To explore how miR-125b loss caused an increase in $CD24^+$ CSC cells resistant to doxorubicin under hypoxia, we compared mRNA profiles between $miR\text{-}125b^{high}$ HCCs and $miR\text{-}125b^{low}$ HCCs. Over 2,000 genes were significantly altered ($P < 0.01$), and the top 15 genes had more than four-fold changes. Four genes (*ASNS* [asparagine synthetase], *S100P, EpCAM*, and *AFP* [alpha-fetoprotein]) expressed at higher levels, while 11 liver metabolism–related genes expressed at lower levels in $miR\text{-}125b^{low}$ HCCs compared with $miR\text{-}125b^{high}$ HCCs (Fig. 4A). EpCAM and AFP are hepatic CSC biomarkers,[31,32] while ASNS and S100P are known to be induced by hypoxia or hypoxia-inducible factor 1 alpha subunit (HIF1α).[33,34] Their differential expression between $miR\text{-}125b^{low}$ HCCs and $miR\text{-}125b^{high}$ HCCs were validated in cohort 3 (Fig. 4B, *EpCAM* in Fig. 3C). The capacity of HIF1α to promote cancer cell stemness has been well documented, and CD24 was also reported to be transcriptionally activated by HIF1α.[35] Thus, miR-125b might regulate HIF1α, which alters the $CD24^+$ cell population.

Overexpressed miR-125b in Huh7 cells reduced the basal level of HIF1α protein moderately (Fig. 4C). When HCC cells were cultured under hypoxia conditions or exposed to $CoCl_2$, HIF1α protein was stabilized (Supporting Fig. S4A,B and Fig. 4C), while overexpressed miR-125b dramatically decreased the induced HIF1α protein (Fig. 4C). As a control, miR-125b did not reduce the level of HIF2α (Supporting Fig. S4C), nor did hypoxia induce miR-125b (Supporting Fig. S4D). Consistent data were observed in HLE cells, as HLE^{125bKO} cells retained a higher level of HIF1α compared with HLE^{WT} cells (Fig. 4C). Furthermore, five well-known HIF1α targets were significantly induced by hypoxia, whereas miR-125b overexpression reduced their basal levels in normoxic conditions and attenuated their induction by hypoxia (Fig. 4D). *In vivo,* miR-125b expression was lower in patients with activation of the HIF1α pathway marked by a group of known HIF1a target genes (Supporting Fig. S4E,F).

HIF1α inhibitor, PX-478, was used to test whether suppressing HIF1α could sensitize HCC cells to doxorubicin under hypoxia. In HCC cells, PX-478 significantly reduced HIF1α protein in a dose-dependent manner (Fig. 4E). Both HuH7 and HLE cells pretreated with PX478 exhibited a significantly reduced cell viability after exposure to doxorubicin under hypoxia.

Under hypoxic condition, $CD24^+$ cells were mostly enriched among the detected different hepatic CSC subpopulations in two HCC cell lines (Fig. 4F). The $EpCAM^+$ population was slightly enriched, whereas hypoxia did not appear to increase the $CD133^+$ cells, but even reduced the $CD44^+$ population. Together, these data indicate that HIF1α protein was accumulated in HCC cells with low levels of miR-125b, which led to a pseudohypoxic status of HCC cells and a subsequent increased $CD24^+$ cell population.

MiR-125b ATTENUATED HIF1α THROUGH BINDING HIF1A INTERNAL RIBOSOME ENTRY SITE AND TARGETING YB-1

HIF1α can be regulated at three levels, including transcription, translation, and protein stability (Fig. 5A). We found that overexpressed miR-125b suppressed neither *HIF1A* mRNA expression (Supporting Fig. S5A) nor its protein stability (Supporting Fig. S5B), indicating that miR-125b might attenuate HIF1α by inhibiting its translation. Under both normoxic and hypoxic conditions, the internal ribosome entry site (IRES) on *HIF1A* 5′ untranslated region (UTR) allowed an efficient translation.[36] YB-1 directly bound to the 5′-UTR of HIF1α, enhancing its translation.[37]

Sequence alignment revealed two potential miR-125b binding sites in the *HIF1A* IRES site (Fig. 5A). A series of bicistronic dual-luciferase reporters (pBiCis reporter) was then constructed to investigate the role of miR-125b on HIF1α translation by binding to the *HIF1A* IRES region. In these constructs, including pBiCis-control, $pBiCis\text{-}IRES^{WT}$, $pBiCis\text{-}IRES^{MT125\#1}$, $pBiCis\text{-}IRES^{MT125\#2}$ and $pBiCis\text{-}IRES^{MT125s}$, the Firefly reporter was transcribed with Renilla but its translation was driven from the different IRES inserts (Fig. 5A,B). When pBiCis reporters bore a wild-type (WT) HIF1α IRES, Firefly luciferase activity was remarkably induced, which was furthermore significantly decreased by miR-125b (Fig. 5B). When miR-125b binding site 1 was mutated in the HIF1α IRES region, this mutated IRES still led to an induced Firefly reporter activity, whereas

overexpressed miR-125b was no longer able to suppress the induced luciferase activity. However, miR-125b binding site 2 did not appear to present such an effect (Fig. 5B). In addition, when Ago-1 (but not other Agos) was silenced, miR-125b was not capable of reducing the Firefly reporter activity driven by *HIF1A* IRES anymore (Fig. 5C). These indicated that miR-125b influenced the function of *HIF1A* IRES on enhancing its translation by binding to the miR-125b binding site 1 in an Ago-1-dependent manner.

The binding region of YB-1 was about 120 bp next to the transcription start site of *HIF1A* (Fig. 5A). Consistently, silencing YB-1 led to decreased protein levels of HIF1α in two HCC cell lines, especially under hypoxic condition (Fig. 5D and Supporting Fig. S5C,D). The 3′UTR region of *YBX1* (encoding YB-1) contains one miR-125b binding site (Fig. 5E). Overexpressed miR-125b reduced the level of YB-1 protein and HIF1α, while forced expression of YB-1 rescued the miR-125b-supressed HIF1α level (Fig. 5D). When the miR-125b binding sequence in *YBX1* 3′-UTR was present, forced expression of miR-125b significantly decreased the luciferase activity (Fig. 5E). This effect was absent after mutation of the partial corresponding miR-125b binding site. Therefore, miR-125b targets *YBX1* by binding to the 3'UTR region of *YBX1,* contributing to HIF1α translation. Furthermore, silencing YB-1 also reduced the *HIF1A* IRES activity significantly under either normoxic or hypoxic condition, and overexpressed miR-125b together with silencing YB-1 further reduced the *HIF1A* IRES activity (Fig. 5F). These data demonstrate that miR-125b could suppress *HIF1A* translation through cap-independent manners (i.e., directly binding its IRES region and by targeting YB-1).

MiR-125b LOSS ENHANCED AN AUTOCRINE HIF1α/PDGFβ/AKT LOOP TO ACCUMULATE HIF1α BY TARGETING PDGFβ RECEPTOR

It was shown previously that PI3K-AKT signaling promoted *HIF1A* translation through a mRNA cap-dependent manner.[38] Interestingly, a higher level of miR-125b was related to a lower level of phosphorylated AKT in Huh7 and HLE cells (Supporting Fig. S6A). However, none of the key AKT pathway proteins was predicted as miR-125b target. Several growth factors have been demonstrated to be induced by HIF1α under hypoxia, activating the PI3K-AKT signaling pathway, through which a positive autocrine loop formed (thus, further increasing HIF1α protein).[39,40] Hence, we examined some of these factors and found seven HIF1α-targeted growth factors to be significantly induced by hypoxia. Among them, *PDGFB, EPO,* and *IGF2* (insulin-like growth factor 2) levels were increased by more than five-fold in Huh7 or HLE cells (Fig. 6A and Supporting Fig. S6B). EPO in breast cancer and IGF2 in skeletal myogenesis have been reported to be miR-125b target genes.[41,42] PDGFRB, encoding the receptor of PDGFβ, contained a predicted miR-125b binding site in its coding region (Fig. 6A). Moreover, PDGFβ induced phosphorylation of AKT-Ser473 significantly in a dose-dependent manner, whereas IGF2 or EPO did not (Fig. 6B and Supporting Fig. S6C). In both Huh7 and HLE cells, PDGFβ exerted its activation function on AKT pathway in a short time (Fig. 6C).

We further found that PDGFRB was a *bona fide* target of miR-125b. Overexpressed miR-125b reduced *PDGFRB* mRNA level in Huh7 cells (Supporting Fig. S6D). Compared with HLE^{WT} cells, HLE^{125bKO} exhibited a higher level of PDGFRB, which could be

reduced by overexpressed miR-125b (Fig. 6D). As shown in Fig. 6E, when the WT miR-125b binding sequence in *PDGFRB* but not the mutated form one was present, forced expression of miR-125b decreased the luciferase activity. In addition, PDGFRB overexpression partially rescued the inhibition of miR-125b on HIF1α (Fig. 6F). Thus, loss of miR-125b also enhanced an autocrine regulatory loop, HIFα/PDGFβ/PDGFRB/AKT, to accumulate HIF1α. Together, HIF1α translation was tightly regulated by miR-125b, not only through targeting its IRES region and YB-1, but also suppressing PDGFRB to manage an autocrine loop of accumulating HIF1α.

CD24 AND EPO, KEY MiR-125b/HIF1α-AXIS TARGETS, RELATED TO HCC POOR PROGNOSIS AFTER TACE

Both miR-125 loss and hypoxia treatment significantly enriched the $CD24^{+}$ cell population, which exhibited strong resistance to doxorubicin under hypoxia. Moreover, *CD24* expression level in HCCs was negatively correlated with miR-125b in both cohort 1 and 3 (Fig. 7A). In cohort 1, patients were grouped to $CD24^{High}$ and $CD24^{Low}$ cases based on the *CD24* median cutoff in HCCs, and patients with $CD24^{Low}$ HCC exhibited a significant survival benefit from adjuvant TACE compared to patients with $CD24^{High}$ (Fig. 7B). As a control, CD24 level was not related to HCC prognosis in patients without TACE therapy. We further performed immunohistochemistry (IHC) for CD24 in 60 FFPE HCC tumors from cohort 2 (Fig. 7C). As shown in Fig. 7D, in patients with adjuvant TACE, the CD24 IHC staining score was significantly higher in tumors from HCCs with recurrence compared to those without recurrence. Such a difference was not noticed in patients without TACE. Consistently, the higher the CD24 IHC score was, the lower the miR-125b level was. Survival analysis revealed that patients with HCC with weak or negative CD24 staining (score ≤ 4) gained significant survival benefit from adjuvant TACE therapy compared to patients with strong CD24 staining (score ≥ 6) (Fig. 7E).

EPO is a well-known HIF1α target gene and a putative target of miR-125b.[41,43] In Huh7 cells, overexpressed miR-125b reduced the level of *EPO* mRNA, EPO protein, and secreted EPO in a dose-dependent manner (Fig. 8A and Supporting Fig. S7A). Consistent data were obtained in HLE (Supporting Fig. S7B). When cells were under hypoxia, *EPO* mRNA was significantly induced in a time-dependent manner, while forced expression of miR-125b also significantly reduced the hypoxia-induced EPO (Fig. 8B). Even more significantly, the secreted-EPO induced by hypoxia could fade away when introducing miR-125b expression. *In vivo, EPO* level in HCCs was negatively correlated with miR-125b in both cohorts 1 and 3 (Fig. 8C). These results indicated that EPO was strongly related to the low level of miR-125b and to HIF1α activation.

In cohort 1, patients with EPO^{Low} HCC, compared to patients with EPO^{High}, obtained significant survival benefit from adjuvant TACE after tumor resection, evident by a longer overall survival time and a prolonged time to recurrence (Fig. 8D). As a control, EPO levels were not related to HCC prognosis in patients without TACE therapy.

As a secretory glycoprotein, EPO naturally holds a great clinical potential to preselect patients with HCC for TACE if the EPO level in blood could consistently associate with the prognosis of patients with HCC after TACE. We then recruited 11 patients in cohort

4 with primarily BCLC-B stage HCCs and having TACE as their first-line therapy. Their plasma samples were collected before TACE. Consistently, patients with high plasma EPO levels did not respond well to TACE (Fig. 8E). Patient 1 with the highest EPO level died in a month following TACE therapy. Patients 2-4 had relative high EPO levels, and all of them had disease progression after TACE based on mRECIST assessment. Seven patients (5-11) presented low-plasma EPO levels and were all alive following TACE therapy. Based on mRECIST assessment, 4 of these patients presented partial response, 2 patients were in a stable disease stage, while only 1 showed disease progression after TACE treatment. These results indicate EPO as the indicator of miR-125b/HIF1α axis, holding the potential as a noninvasive biomarker to guide patients for choosing TACE therapy, and the specificity of miR-125b/HIF1α axis in regulating cell response to TACE.

Discussion

Currently, at least 30% of the entire HCC population could potentially receive TACE therapy in the course of their disease. However, the survival benefits of patients managed with this technique are variable. The current precision medicine era was led by accumulating knowledge in “omics.” As TACE is mostly applied in advanced-stage patients, one of the key hurdles is deficiency in tissue specimens before TACE from a large population to perform the omics-related research. In Asia, adjuvant TACE was also used to prevent metastasis after tumor resection, and such a clinical practice allowed us to analyze the tissue bio-specimens before TACE therapy with the goal of identifying key biological markers or pathways involved in effective response to TACE therapy.

In this study, we gathered two HCC cohorts with adjuvant TACE after tumor resection. A miRNA-signature was identified and related to HCC recurrence only in patients with adjuvant TACE. MiR-125b, the top candidate of this signature, was associated with HCC cell sensitivity to an *in vitro* TACE-mimic treatment through regulating *HIF1A* translation. MiR-125b attenuated HIF1α translation using three divergent angles: influencing *HIF1A* IRES activity, suppressing YB-1, and attenuating an autocrine loop (HIF1α/PDGFβ/pAKT/HIF1α) by targeting PDGFβ receptor. Thus, miR-125b functioned as a key suppressor of HIF1α. In miR-125b^{low} HCCs, HIF1α accumulated and led to a pseudohypoxia environment, contributing to HCC resistance to TACE.

It is widely reported that HIF1α could promote cancer stemness. Here we evaluated the enrichment of four different CSC subpopulations under hypoxic condition and noticed a specifically high enrichment of the CD24^{+} subpopulation in HCC cells. Strikingly, compared with other CSC biomarkers, CD24^{+} subpopulations exhibited the strongest resistance to an *in vitro* TACE-mimic treatment, while CD24^{-} subpopulations were most sensitive among all of the examined subpopulations. Therefore, a pseudohypoxia environment in miR-125b^{low} HCCs produced an enriched CD24^{+} population, which resulted in resistance to doxorubicin under hypoxia. These results also implied the distinct response of CSC populations to variable cell environments, illustrating a strong need for a thorough and careful design of CSC-related research.

Some groups reported that patients with MVI in their resected HCCs gained survival benefit from adjuvant TACE after tumor resection,[29] which we also noticed in our cohort 2. However, the controversial data also revealed that the absence of MVI was associated with improved survival for patients with HCC with adjuvant TACE.[28] Thus, well-designed and controlled analyses in a large cohort are needed to reach a solid conclusion on the role of MVI in assisting one to choose adjuvant TACE for patients with HCC. In addition, MVI is currently detected by postoperative histological examination, which limits its use for preoperative assessment of prognosis as well as for patients being given nonsurgical treatments. In our study, high levels of miR-125b and low levels of CD24 and EPO were related to prolonged survival and time to recurrence for patients with adjuvant TACE, respectively. Among them, EPO is a secreted protein. Low-plasma EPO was also associated with a better response to TACE in a small set of patients with BCLC-B HCC who had TACE as their first-line therapy. In addition, we noticed a liver-specific expression of EPO. In comparison to 16 different human adult normal organs, liver expressed the highest level of EPO mRNA, and GTEx data showed similar results (Supporting Fig. S7C). Consistently, secreted EPO protein and EPO mRNA were higher in HCC cell lines compared with other cancer lines (Supporting Fig. S7D). These together indicate the possibility and advantage of using EPO as a potential biomarker in HCC. Our ongoing prospective clinical studies in patients at different BCLC stages with TACE will further clarify the clinical interest of the miR-125b/CD24/EPO predictive panel, especially the value of EPO as a plasma indicator.

Both HIF1α and miR-125b have been shown to contribute to HCC progression. The activated HIF1α pathway is involved in HCC angiogenesis and metastasis[44] and miR-125b-suppressed epithelial mesenchymal transition, tumor growth, migration, and invasion by targeting Smad2/4 and TRAF6 in HCC.[17,18] Interestingly, serum exosomal miR-125b, but not whole-serum miR-125b, predicted HCC outcome.[45] Our results also showed that miR-125b suppressed spheroid formation and the CSC population in HCC cell lines, although the miR-125b level in HCC tissues of cohorts 1 and 2 showed no significant relation with prognosis of HCC cases without TACE. Therefore, it is possible that HCC tissue miR-125b, serum miR-125b, and exosomal miR-125b might exhibit different levels and/or have different roles in prognosis prediction. Tissue miR-125b might generally suppress tumor progression in patients with HCC, while the pseudohypoxia environment caused by loss of miR-125b in HCC tissue reflected the HCC cell sensitivity status to TACE therapy.

In summary, the miR-125b/HIF1α axis acts as a key pathway related to HCC cell sensitivity to TACE treatment and might guide patients with HCC in choosing TACE therapy. Our work paves the way of moving TACE therapy toward a precision stage, with the hope of largely improving the outcome of patients with HCC.

Supplementary Material

Refer to Web version on PubMed Central for supplementary material.

Acknowledgment:

The authors thank the core facility in the Life Sciences Institute for their support on the fluorescence-activated cell-sorting analysis.

Supported by the National Key R&D Program of China (2018YFA0800504 to J.J.), Zhejiang Basic Public Welfare Research Program (LZ20H160003 to J.J.), National Natural Science Foundation of China (81874054 and 81672905 to J.J.), Fundamental Research Funds for the Central Universities in China (to J.J.), Thousand Young Talents Plan of China (to J.J.), National Natural Science Foundation of China (30801383 and 81472713 to L.Z.), German Research Foundation (314905040 and TRR 209 Liver Cancer Subproject B01 to S.R.), and the Intramural Program of the Center for Cancer Research, National Cancer Institute of the United States (X.W.W.).

Abbreviations:

AFP	alpha-fetoprotein
ASNS	asparagine synthetase
BCLC	Barcelona Clinic Liver Cancer
CSC	cancer stem cell
EpCAM	epithelial cell adhesion molecule
EPO	erythropoietin
FFPE	formalin-fixed paraffin-embedded
HCC	hepatocellular carcinoma
IGF2	insulin-like growth factor 2
IHC	immunohistochemistry
IRES	internal ribosome entry site
miR-125b	miR-125b-5p
mRECIST	modified Response Evaluation Criteria in Solid Tumors
mRNA	messenger RNA
MVI	microvascular invasion
pBiCis reporter	bicistronic dual-luciferase reporters
TACE	transarterial chemoembolization
UTR	untranslated region
WT	wild type

REFERENCES

1). Siegel RL, Miller KD, Jemal A. Cancer statistics, 2019. CA Cancer J Clin 2019;69:7–34. [PubMed: 30620402]

2). Llovet JM, Zucman-Rossi J, Pikarsky E, Sangro B, Schwartz M, Sherman M, et al. Hepatocellular carcinoma. Nat Rev Dis Primers 2016;2:16018. [PubMed: 27158749]

3). Forner A, Gilabert M, Bruix J, Raoul J-L. Treatment of intermediate-stage hepatocellular carcinoma. Nat Rev Clin Oncol 2014;11:525–535. [PubMed: 25091611]

4). Habib A, Desai K, Hickey R, Thornburg B, Lewandowski R, Salem R. Transarterial approaches to primary and secondary hepatic malignancies. Nat Rev Clin Oncol 2015;12:481–489. [PubMed: 25985939]

5). Bargellini I, Bozzi E, Campani D, Carrai P, De Simone P, Pollina L, et al. Modified RECIST to assess tumor response after transarterial chemoembolization of hepatocellular carcinoma: CT-pathologic correlation in 178 liver explants. Eur J Radiol 2013;82:e212–e218. [PubMed: 23332890]

6). Nishikawa H, Arimoto A, Wakasa T, Kita R, Kimura T, Osaki Y. Effect of transcatheter arterial chemoembolization prior to surgical resection for hepatocellular carcinoma. Int J Oncol 2013;42:151–160. [PubMed: 23174998]

7). Zhou Y, Zhang X, Wu L, Ye F, Su X, Shi L, et al. Meta-analysis: preoperative transcatheter arterial chemoembolization does not improve prognosis of patients with resectable hepatocellular carcinoma. BMC Gastroenterol 2013;13:51. [PubMed: 23509884]

8). Li KW, Li X, Wen TF, Lu WS. The effect of postoperative TACE on prognosis of HCC: an update. Hepatogastroenterology 2013;60:248–251. [PubMed: 23574651]

9). Sun HC, Tang ZY. Preventive treatments for recurrence after curative resection of hepatocellular carcinoma—a literature review of randomized control trials. World J Gastroenterol 2003;9:635–640. [PubMed: 12679900]

10). Bruix J, Sala M, Llovet JM. Chemoembolization for hepatocellular carcinoma. Gastroenterology 2004;127:S179–S188. [PubMed: 15508083]

11). Wong CM, Tsang FH, Ng IO. Non-coding RNAs in hepatocellular carcinoma: molecular functions and pathological implications. Nat Rev Gastroenterol Hepatol 2018;15:137–151. [PubMed: 29317776]

12). Ji J, Shi J, Budhu A, Yu Z, Forgues M, Roessler S, et al. MicroRNA expression, survival, and response to interferon in liver cancer. N Engl J Med 2009;361:1437–1447. [PubMed: 19812400]

13). Ji J, Yu L, Yu Z, Forgues M, Uenishi T, Kubo S, et al. Development of a miR-26 companion diagnostic test for adjuvant interferon-alpha therapy in hepatocellular carcinoma. Int J Biol Sci 2013;9:303–312. [PubMed: 23569435]

14). Lee RC, Feinbaum RL, Ambros V. The C. elegans heterochronic gene lin-4 encodes small RNAs with antisense complementarity to lin-14. Cell 1993;75:843–854. [PubMed: 8252621]

15). Wightman B, Ha I, Ruvkun G. Posttranscriptional regulation of the heterochronic gene lin-14 by lin-4 mediates temporal pattern formation in C. elegans. Cell 1993;75:855–862. [PubMed: 8252622]

16). Sun YM, Lin KY, Chen YQ. Diverse functions of miR-125 family in different cell contexts. J Hematol Oncol 2013;6:6. [PubMed: 23321005]

17). Xie C, Zhang LZ, Chen ZL, Zhong WJ, Fang JH, Zhu Y, et al. A hMTR4-PDIA3P1-miR-125/124-TRAF6 regulatory axis and its function in NF kappa B signaling and chemoresistance. HEPATOLOGY 2020;71:1660–1677. [PubMed: 31509261]

18). Zhou JN, Zeng Wang Q, Zhang B, Li ST, Nan X, et al. MicroRNA-125b attenuates epithelial-mesenchymal transitions and targets stem-like liver cancer cells through small mothers against decapentaplegic 2 and 4. HEPATOLOGY 2015;62:801–815. [PubMed: 25953743]

19). Budhu A, Jia HL, Forgues M, Liu CG, Goldstein D, Lam A, et al. Identification of metastasis-related microRNAs in hepatocellular carcinoma. HEPATOLOGY 2008;47:897–907. [PubMed: 18176954]

20). Roessler S, Long EL, Budhu A, Chen Y, Zhao X, Ji J, et al. Integrative genomic identification of genes on 8p associated with hepatocellular carcinoma progression and patient survival. Gastroenterology 2012;142:957–966.e912. [PubMed: 22202459]

21). Roessler S, Jia HL, Budhu A, Forgues M, Ye QH, Lee JS, et al. A unique metastasis gene signature enables prediction of tumor relapse in early-stage hepatocellular carcinoma patients. Cancer Res 2010;70:10202–10212. [PubMed: 21159642]

22). Gu Y, Wei X, Sun Y, Gao H, Zheng X, Wong LL, et al. miR-192-5p Silencing by genetic aberrations is a key event in hepatocellular carcinomas with cancer stem cell features. Cancer Res 2019;79:941–953. [PubMed: 30530815]

23). Sun Y, Ji F, Kumar MR, Zheng X, Xiao Y, Liu N, et al. Transcriptome integration analysis in hepatocellular carcinoma reveals discordant intronic miRNA-host gene pairs in expression. Int J Biol Sci 2017;13:1438–1449. [PubMed: 29209147]

24). Takayasu K, Arii S, Ikai I, Omata M, Okita K, Ichida T, et al. Prospective cohort study of transarterial chemoembolization for unresectable hepatocellular carcinoma in 8510 patients. Gastroenterology 2006;131:461–469. [PubMed: 16890600]

25). Llovet JM, Real MI, Montana X, Planas R, Coll S, Aponte J, et al. Arterial embolisation or chemoembolisation versus symptomatic treatment in patients with unresectable hepatocellular carcinoma: a randomised controlled trial. Lancet 2002;359:1734–1739. [PubMed: 12049862]

26). Villanueva A, Hernandez-Gea V, Llovet JM. Medical therapies for hepatocellular carcinoma: a critical view of the evidence. Nat Rev Gastroenterol Hepatol 2013;10:34–42. [PubMed: 23147664]

27). Alpini G, Glaser SS, Zhang JP, Francis H, Han Y, Gong J, et al. Regulation of placenta growth factor by microRNA-125b in hepatocellular cancer. J Hepatol 2011;55:1339–1345. [PubMed: 21703189]

28). Wang Z, Ren Z, Chen Y, Hu J, Yang G, Yu L, et al. Adjuvant transarterial chemoembolization for HBV-related hepatocellular carcinoma after resection: a randomized controlled study. Clin Cancer Res 2018;24:2074–2081. [PubMed: 29420221]

29). Chen W, Ma T, Zhang J, Zhang X, Chen W, Shen Y, et al. A systematic review and meta-analysis of adjuvant transarterial chemoembolization after curative resection for patients with hepatocellular carcinoma. HPB (Oxford) 2020;22:795–808. [PubMed: 31980307]

30). Ji J, Yamashita T, Budhu A, Forgues M, Jia HL, Li C, et al. Identification of microRNA-181 by genome-wide screening as a critical player in EpCAM-positive hepatic cancer stem cells. HEPATOLOGY 2009;50:472–480. [PubMed: 19585654]

31). Yamashita T, Forgues M, Wang W, Kim JW, Ye Q, Jia H, et al. EpCAM and alpha-fetoprotein expression defines novel prognostic subtypes of hepatocellular carcinoma. Cancer Res 2008;68:1451–1461. [PubMed: 18316609]

32). Ji J, Wang XW. Clinical implications of cancer stem cell biology in hepatocellular carcinoma. Semin Oncol 2012;39:461–472. [PubMed: 22846863]

33). Du F, Chen J, Liu H, Cai Y, Cao T, Han W, et al. SOX12 promotes colorectal cancer cell proliferation and metastasis by regulating asparagine synthesis. Cell Death Dis 2019;10:239. [PubMed: 30858360]

34). Mao X, Wong SY, Tse EY, Ko FC, Tey SK, Yeung YS, et al. Mechanisms through which hypoxia-induced Caveolin-1 drives tumorigenesis and metastasis in hepatocellular carcinoma. Cancer Res 2016;76:7242–7253. [PubMed: 27784747]

35). Thomas S, Harding MA, Smith SC, Overdevest JB, Nitz MD, Frierson HF, et al. CD24 is an effector of HIF-1-driven primary tumor growth and metastasis. Cancer Res 2012;72:5600–5612. [PubMed: 22926560]

36). Wu CA, Huang DY, Lin WW. Beclin-1-independent autophagy positively regulates internal ribosomal entry site-dependent translation of hypoxia-inducible factor 1alpha under nutrient deprivation. Oncotarget 2014;5:7525–7539. [PubMed: 25115400]

37). El-Naggar AM, Veinotte CJ, Cheng H, Grunewald TG, Negri GL, Somasekharan SP, et al. Translational activation of HIF1alpha by YB-1 promotes sarcoma metastasis. Cancer Cell 2015;27:682–697. [PubMed: 25965573]

38). LaGory EL, Giaccia AJ. The ever-expanding role of HIF in tumour and stromal biology. Nat Cell Biol 2016;18:356–365. [PubMed: 27027486]

39). Janku F Phosphoinositide 3-kinase (PI3K) pathway inhibitors in solid tumors: from laboratory to patients. Cancer Treat Rev 2017;59:93–101. [PubMed: 28779636]

40). Lau CK, Yang ZF, Ho DW, Ng MN, Yeoh GC, Poon RT, et al. An Akt/hypoxia-inducible factor-1alpha/platelet-derived growth factor-BB autocrine loop mediates hypoxia-induced

chemoresistance in liver cancer cells and tumorigenic hepatic progenitor cells. Clin Cancer Res 2009;15:3462–3471. [PubMed: 19447872]

41). Ferracin M, Bassi C, Pedriali M, Pagotto S, D'Abundo L, Zagatti B, et al. miR-125b targets erythropoietin and its receptor and their expression correlates with metastatic potential and ERBB2/HER2 expression. Mol Cancer 2013;12:130. [PubMed: 24165569]

42). Ge Y, Sun Y, Chen J. IGF-II is regulated by microRNA-125b in skeletal myogenesis. J Cell Biol 2011;192:69–81. [PubMed: 21200031]

43). Ke S, Chen S, Dong Z, Hong CS, Zhang Q, Tang L, et al. Erythrocytosis in hepatocellular carcinoma portends poor prognosis by respiratory dysfunction secondary to mitochondrial DNA mutations. HEPATOLOGY 2017;65:134–151. [PubMed: 27774607]

44). Chen C, Lou T. Hypoxia inducible factors in hepatocellular carcinoma. Oncotarget 2017;8:46691–46703. [PubMed: 28493839]

45). Liu W, Hu J, Zhou K, Chen F, Wang Z, Liao B, et al. Serum exosomal miR-125b is a novel prognostic marker for hepatocellular carcinoma. Onco Targets Ther 2017;10:3843–3851. [PubMed: 28814883]

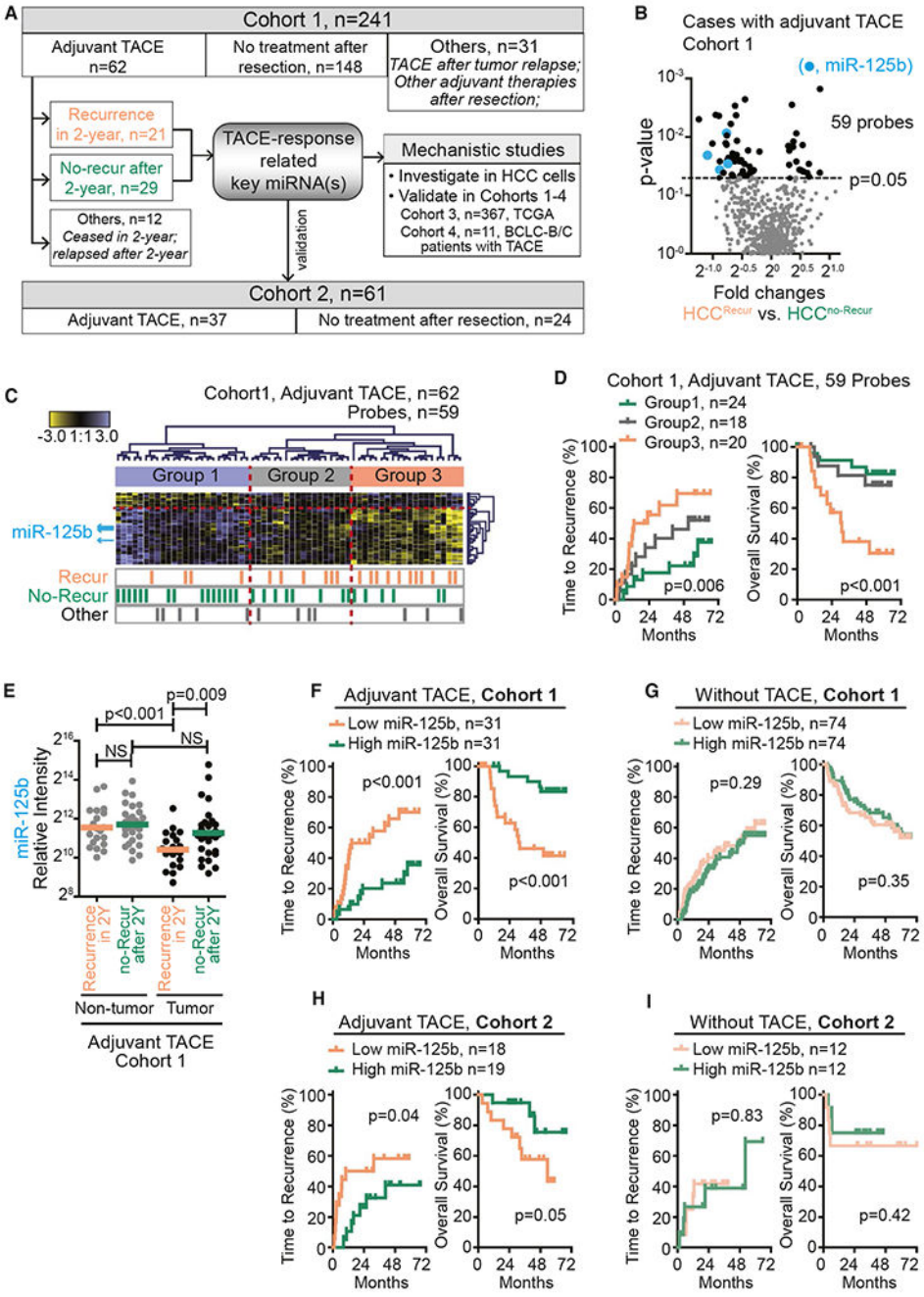

FIG. 1.

MiRNA profiles were different between HCCs with recurrence in 2 years and HCCs without recurrence after 2 years for patients with HCC with adjuvant TACE after resection. (A) The flow chart for screening and studying miRNAs related to tumor progression in the HCC tissues of patients with adjuvant TACE. (B) Scatter plot of miRNA fold changes with *P* values from class comparison analysis between HCC^{Recur} and $HCC^{no\text{-}Recur}$. Fifty-nine miRNA probes had *P* values less than 0.05. Four significant probes refer to miR-125b. (C) Hierarchical clustering of 62 HCC cases with adjuvant TACE based on 59 significant

miRNA probes from (B). Kaplan-Meier analysis of time to recurrence and overall survival for three groups of HCC cases. (D) MiR-125b relative intensity in tumor and nontumor tissues of HCC^{Recur} versus $HCC^{no\text{-}Recur}$ in patients with adjuvant TACE. (E) Kaplan-Meier analysis of time to recurrence and overall survival in HCC cases from cohort 1 based on miR-125b level and adjuvant TACE therapy. (F) Kaplan-Meier analysis of time to recurrence and overall survival in HCC cases in cohort 2 based on miR-125b level and adjuvant TACE therapy. (E,F) The median levels of miR-125b in each group were used as the cutoffs. Log-rank test was performed. Abbreviations: NS, not significant; TCGA, The Cancer Genome Atlas.

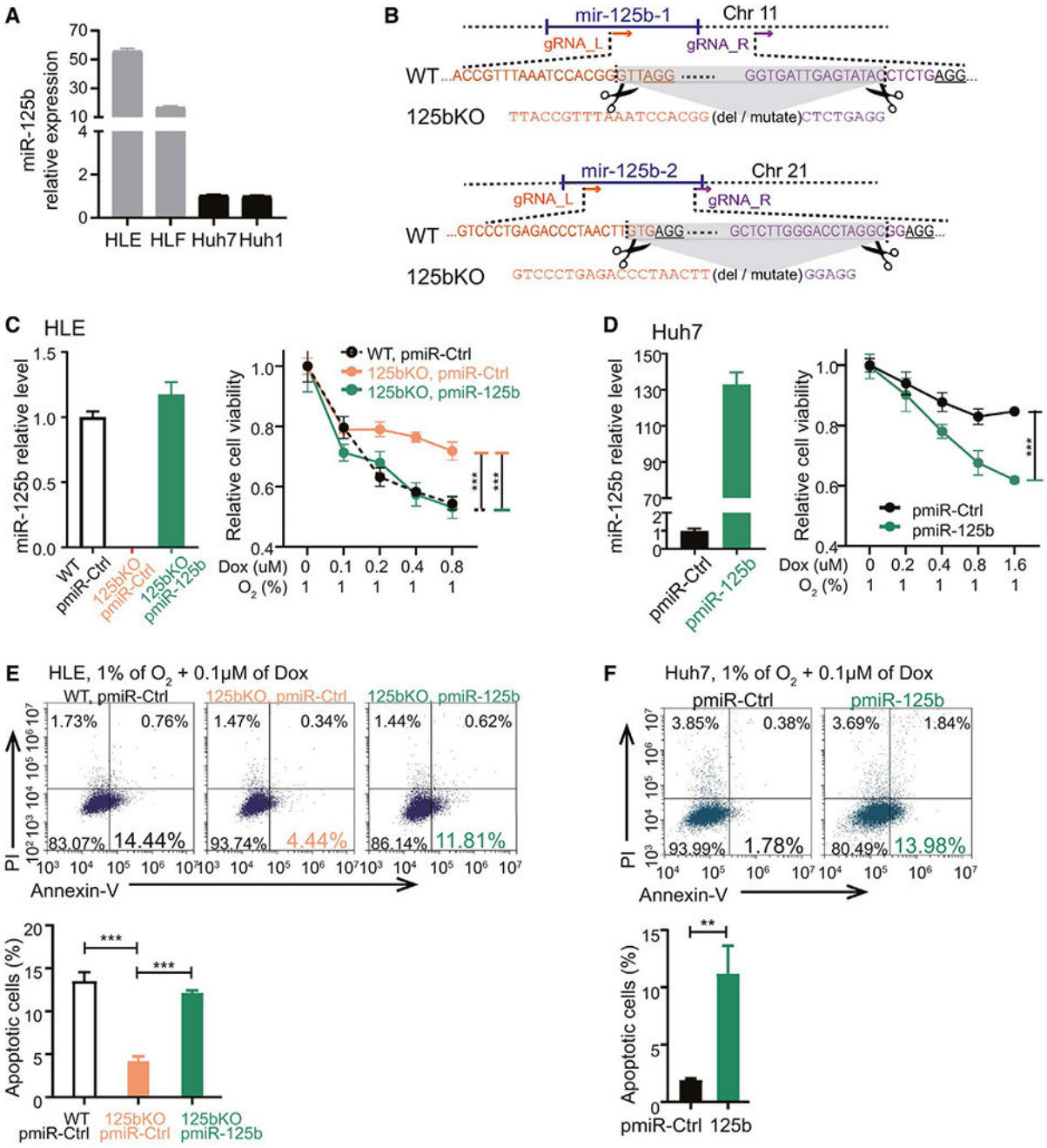

FIG. 2.

HCC cells with miR-125b loss were mimicking *in vivo* TACE therapy. (A) miR-125b expression level in four different HCC cell lines. (B) The schematic structure of WT primary mir-125b-1 and mir-125b-2 as well as miR-125b knockout by CRISPR-CAS9 system. (C,D) Relative cell viability of HLE cells (C) and Huh7 cells (D) with altered expression of miR-125b when they were exposed to the combination of hypoxia and doxorubicin treatment. (E,F) Percentage of apoptotic cells in HLE and Huh7 with altered miR-125b level when exposed to doxorubicin under hypoxia. Abbreviations: gRNA, guide RNA; KO

pmiR-ctrl, miR-125b knockout HLE cells infected with lentivirus pmiR-ctrl; KO pmiR-125, miR-125b knockout HLE cells infected with pmiR-125b; WT pmiR-ctrl, WT HLE cells infected with lentivirus pmiR-ctrl.

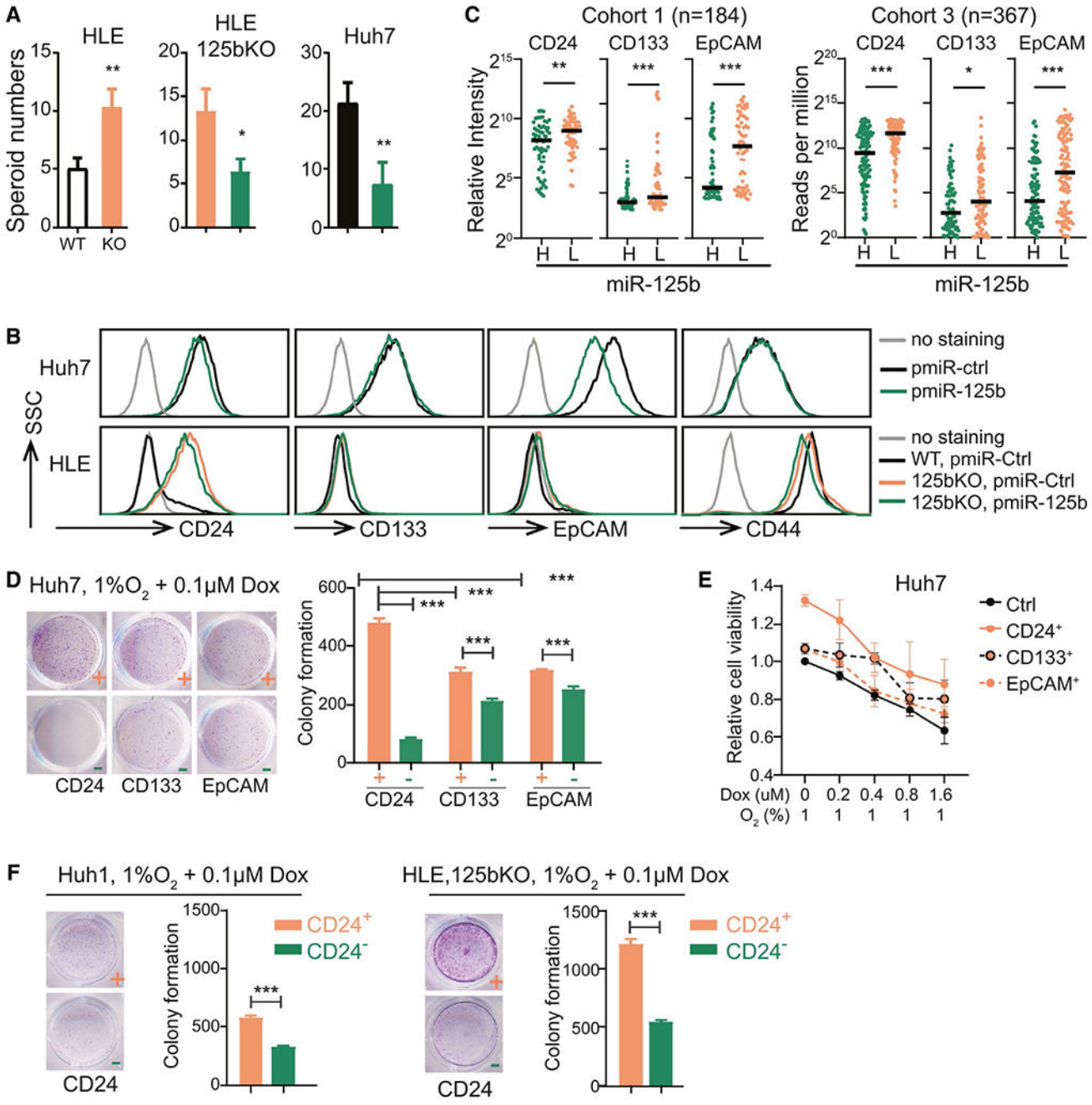

FIG. 3.

Reduced miR-125b led to enrichment of the CD24^{+} CSC population in HCC. (A) Spheroid formation in HLE and Huh7 with altered miR-125b level. Lentivirus pmiR-125b was used to overexpress miR-125b. (B) Flow cytometry analysis was performed in Huh7 and HLE cells with altered miR-125b expression. (C) Relative expression of *CD24*, *CD133*, and *EpCAM* in miR-125b^{high} HCCs and miR-125b^{low} HCCs from the HCC cohort 1 (left) and cohort 3 (right). Unpaired *t* test was used. (D) Colony formation assay of isolated CSC biomarker positive and negative Huh7 cell with exposure to doxorubicin under hypoxia. (E) Relative

cell viability of isolated $CD24^+$, $CD133^+$, and $EpCAM^+$ Huh7 cells following exposure to the combination of hypoxia and doxorubicin treatment. (F) Colony formation assay of isolated $CD24^+$ and $CD24^+$ cells from Huh1 and HLE-125bKO lines with exposure to doxorubicin under hypoxia. Abbreviation: SSC, side scatter. ***P <0.001; **P <0.01; *P < 0.05.

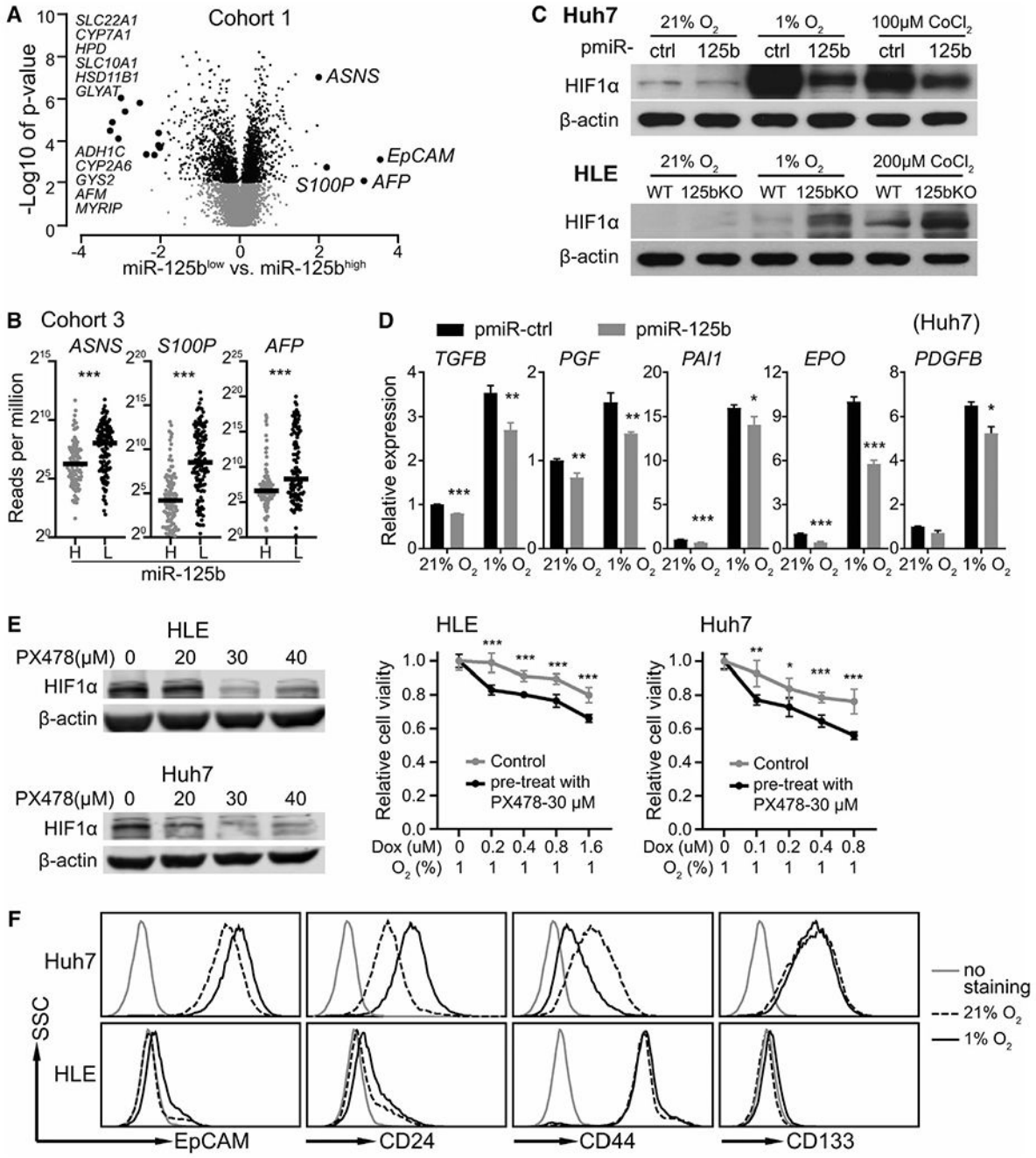

FIG. 4.

HIF1α protein level was increased in HCCs with a low level of miR-125b. (A) Scatter plots of genes that were significantly changed ($P < 0.01$) between miR-125b^{low} HCCs and miR-125b^{high} HCCs in cohort 1. Genes with fold change ≥ 4 were bolded. (B) Reads per million of *ASNS*, *S100P*, and *AFP* in miR-125b^{low} and miR-125b^{high} HCCs from cohort 3. (C) HIF1α protein in Huh7 and HLE cells with altered miR-125b expression. (D) Relative mRNA levels of HIF1α targeting genes in Huh7 cells with or without forced expression of miR-125b under hypoxia (1% O_2) for 24 hours. (E) HIF1α protein expression of HLE/Huh7

cells treated with PX-478. Relative cell viability of HLE/Huh7 cells exposure to doxorubicin under hypoxia after pretreatment with 30 μM of PX-478 for 2 days. (F) Flow cytometry analysis was performed using Huh7 and HLE cells cultured in hypoxia (1% O_2) or normoxic condition. Abbreviation: SSC, side scatter.

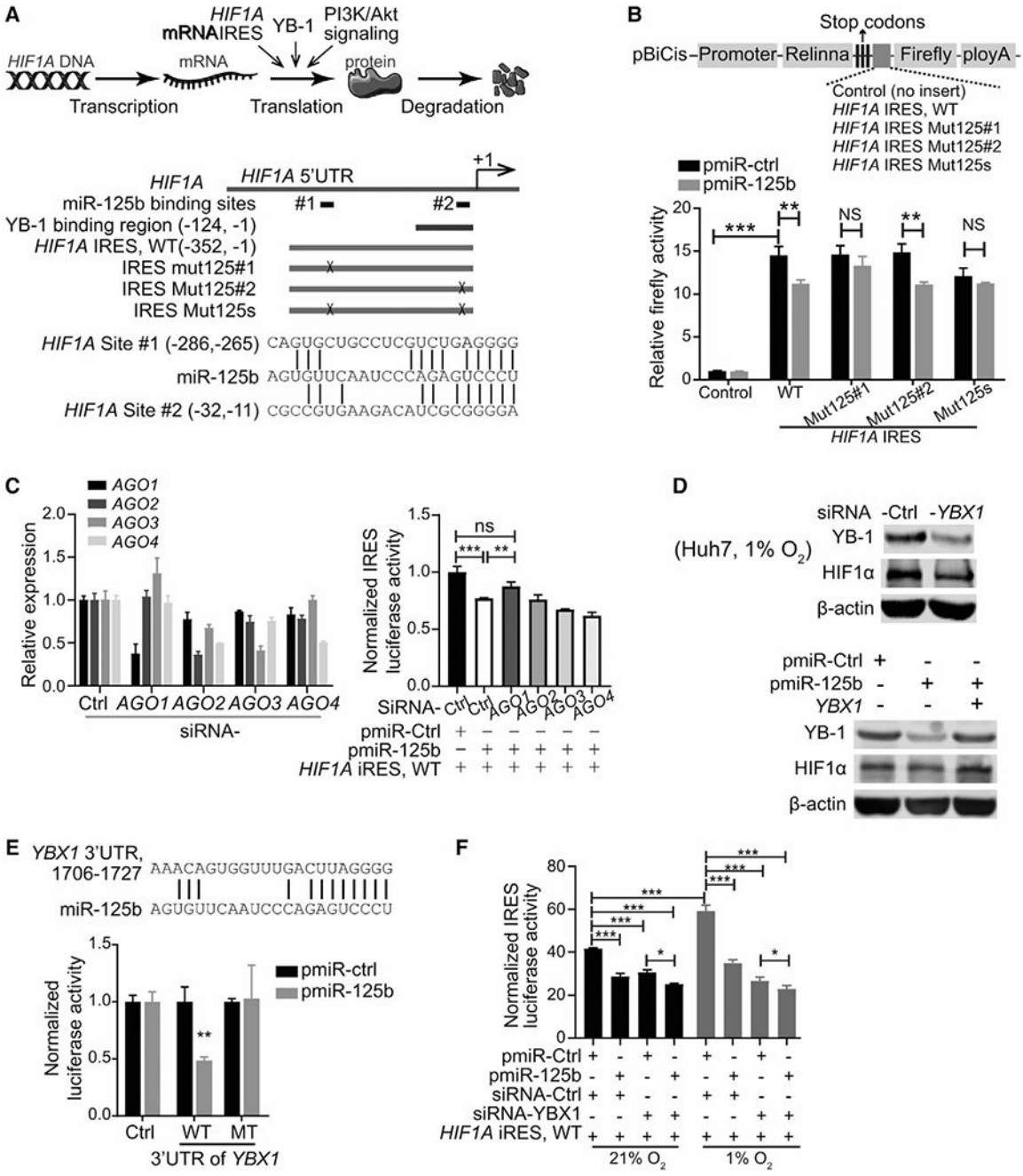

FIG. 5.

miR-125b attenuated *HIF1A* translation by directly inhibiting IRES activity of HIF1α and targeting YB-1. (A) The schematic flow of HIF1a transcription, translation, and protein degradation processes, as well as predicted miR-125b binding sites in the IRES region of HIF1A 5′-UTR. (B) Representative maps of pBiCis-reporter plasmids (top panel). Relative luciferase activity of pBiCis-reporter plasmids in Huh7 cells with or without forced expression of miR-125b (bottom panel). (C) Relative luciferase activity in Huh7 cells with overexpressed miR-125b and silenced AGOs. (D) YB-1 and HIF1α protein expression in

Huh7 cells transfected with siRNA-control and siRNA-*YBX1*, and in Huh7 cells infected with lentivirus miR-125b and transfected with siRNA-*YBX1*. (E) Predicted miR-125b binding site in 3′-UTR of human *YBX1* and relative luciferase activity of reporter plasmids with WT or mutant miR-125b binding site in 3′-UTR of human *YBX1*. (F) Normalized luciferase activity of pBiCis-control and-IRES^{WT} in Huh7 cells infected with lentivirus miR-125b and transfected with siRNA-control and siRNA-*YBX1*. Abbreviations: MT, mutant; ns, not significant; siRNA, small interfering RNA.

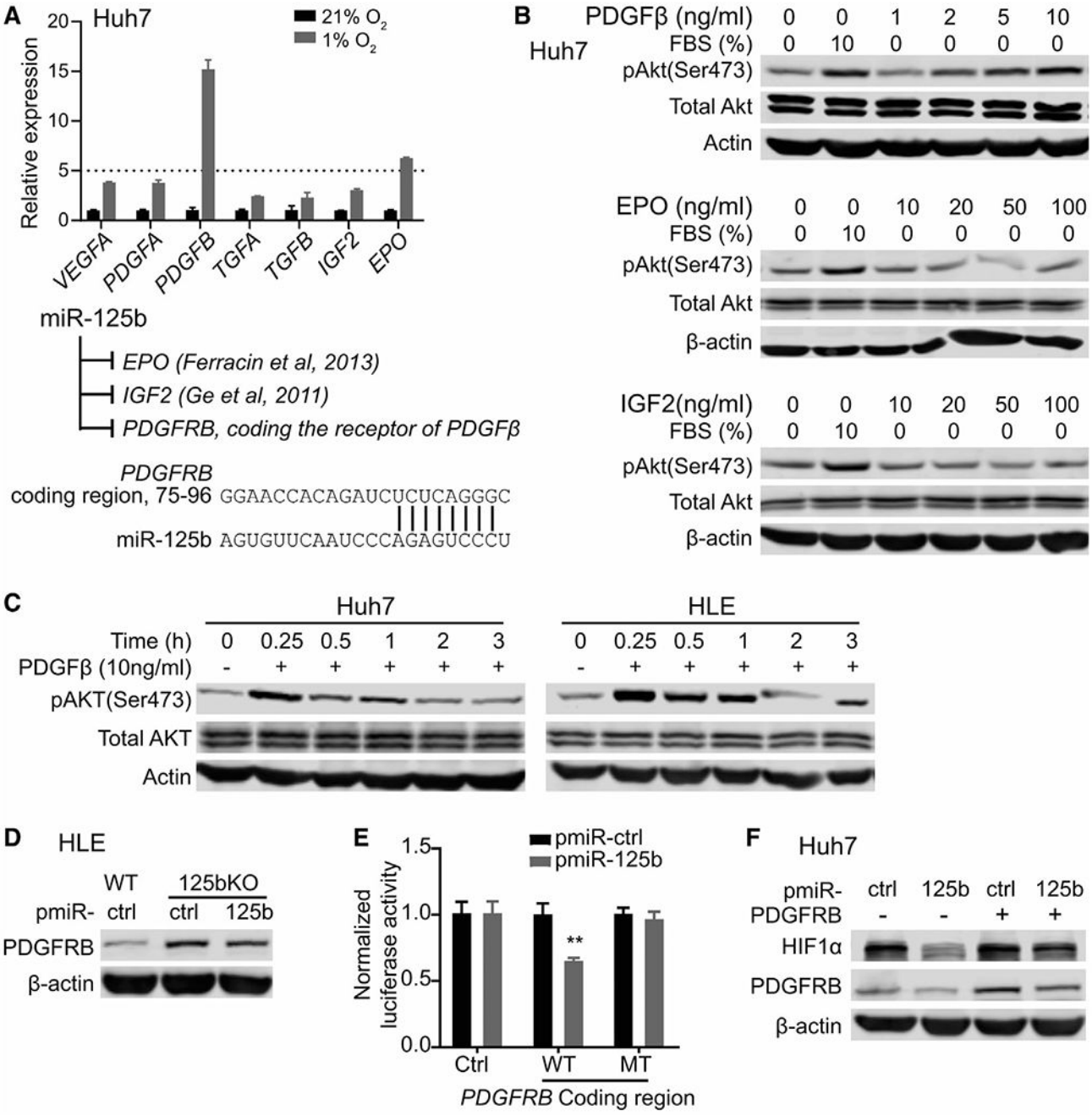

FIG. 6.

miR-125b attenuated HIF1A translation by blocking the AKT pathway by targeting the receptor of HIF1α-induced PDGFβ. (A) Relative expression of HIF1α targeting growth factors (*VEGFA*, *PDGFA*, *PDGFB*, *TGFA*, *TGFB*, *IGF2*, and *EPO*) in HuH7 cells cultured in hypoxia for 24 hours, and possible miR-125b targets of AKT pathway in HCC cells. (B) Phosphorylated AKT (Ser473) and total AKT in Huh7 cells treated with a different dose of PDGFβ, EPO, and IGF2. Fetal bovine serum (10%) was used as positive control to induce phosphorylation of AKT. (C) Phosphorylated AKT (Ser473) and total AKT in Huh7 and

HLE cells treated with PDGFβ for different times. (D) PDGFRB protein level in HLE cells with different levels of miR-125b. (E) Relative Firefly luciferase activity in Huh7 cells using reporter plasmid with miR-125b binding site of PDGFRB in the 3'-UTR region of luciferase vector. (F) PDGFRB and HIF1α protein expression in Huh7 cells with altered level of miR-125b and PDGFRB. Abbreviations: MT, mutant; TGFA/B, transforming growth factor A/B; VEGFA, vascular endothelial growth factor type A.

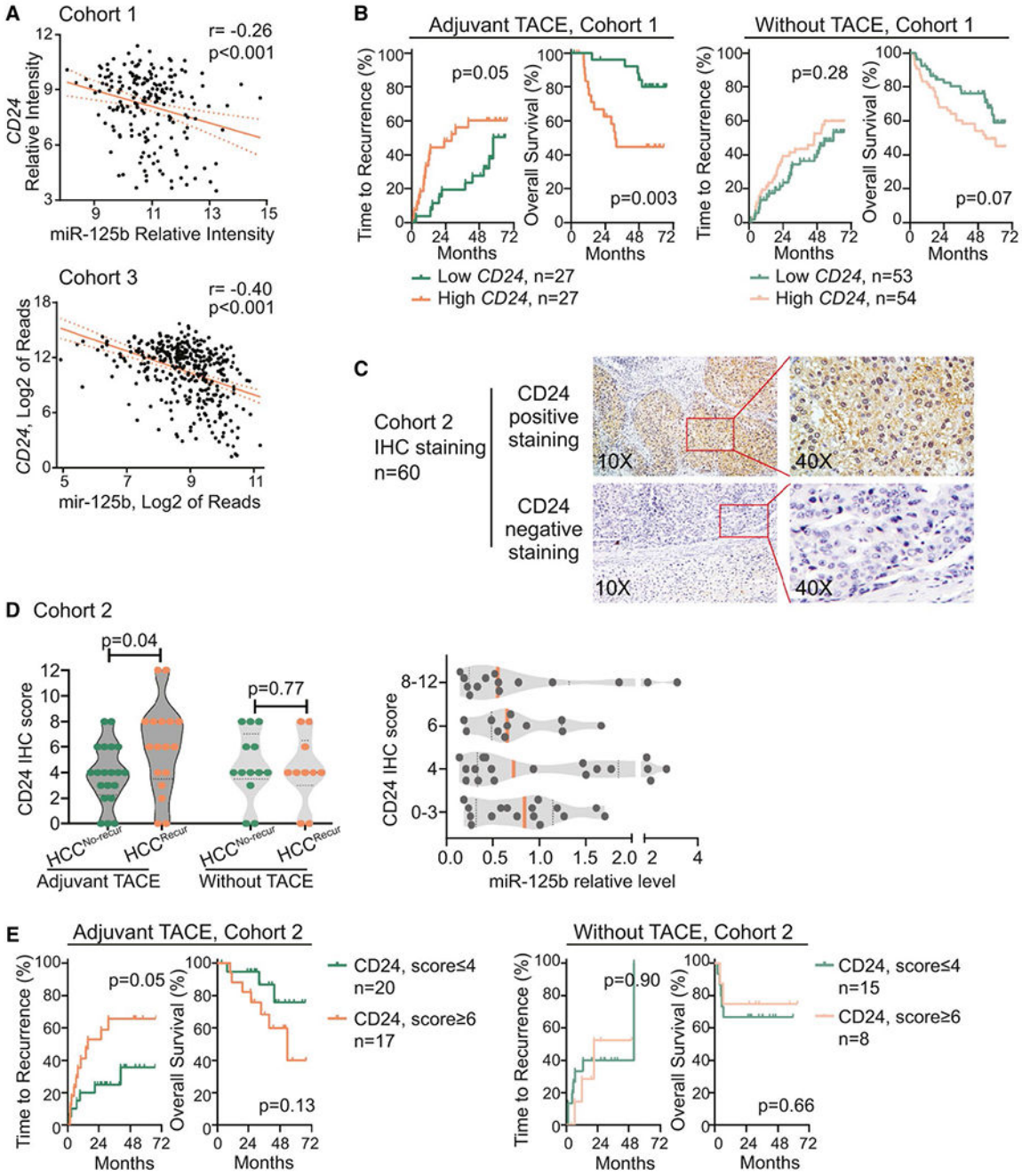

FIG. 7.

Increased CD24 levels were associated with poor prognosis of patients with adjuvant TACE. (A) Pearson correlation of miR-125b with *CD24* in the HCCs of cohort 1 and cohort 3. (B) Kaplan-Meier analysis of time to recurrence and overall survival in HCC cases in cohort 1 based on the *CD24* mRNA level in HCCs and TACE therapy. Log-rank test was performed. (C) Representative picture of CD24 IHC staining in cohort 2. (D) CD24 IHC score in HCC^{Recur} and $HCC^{no\text{-}Recur}$ tumors from patients with/without adjuvant TACE in cohort 2 (left) and relative miR-125b levels in HCCs with different CD24 IHC scores (right). (E)

Kaplan-Meier analysis of time to recurrence and overall survival in HCC cases in cohort 2 based on the CD24 IHC score in HCCs and TACE therapy.

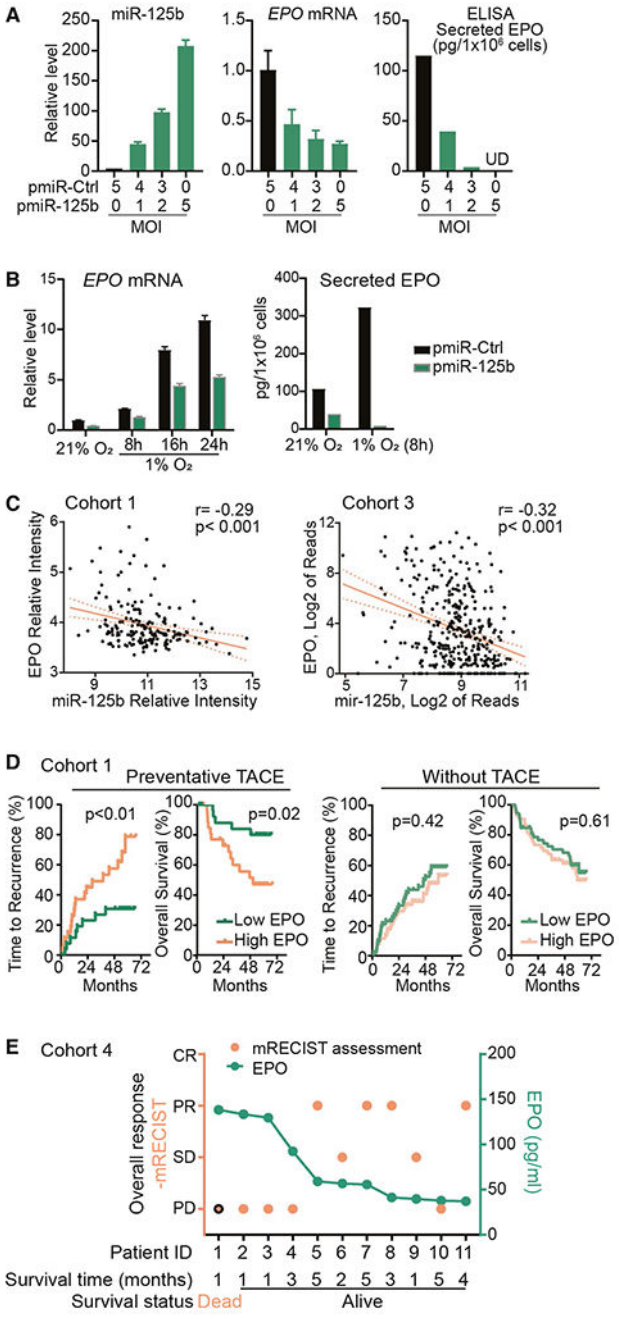

FIG. 8.

Increased EPO levels were associated with poor prognosis of patients with HCC with TACE. (A) Relative levels of miR-125b-5p, *EPO* mRNA, and secreted EPO protein in Huh7 cells infected with one, two, or five multiplicities of infection of miR-125b lentivirus. (B) Relative level of *EPO* mRNA in Huh7 cells infected with five multiplicities of infection of miR-125b lentivirus. (C) Pearson correlation of miR-125b-5p and EPO in HCC tumor tissues of cohorts 1 and 3. (D) Kaplan-Meier analysis of time to recurrence and overall survival in HCC cases in cohort 1 based on the *EPO* mRNA level in HCCs and TACE

therapy. Log-rank test was performed. (E) The relationship of plasma EPO before TACE with overall response to TACE of patients with HCC in cohort 4. mRECIST assessment was used based on computed tomography or magnetic resonance imaging results. Abbreviations: CR, complete response; ELISA, enzyme-linked immunosorbent assay; MOI, multiplicity of infection; PD, progressive disease; PR, partial response; SD, stable disease; UD, under detectable.